Lab Invest 103 (2023) 100256

LABORATORY INVESTIGATION

journal homepage: https://laboratoryinvestigation.org/

Research Article

Engineered Knockout of TRPA1 Inhibits Laser-Induced Choroidal Neovascularization Along With Associated TGFβ1 Expression and Neutrophil Infiltration

Yuta Usui[a], Hiroki Iwanishi[a,*], Takayoshi Sumioka[a], Kana Ichikawa[a], Masayasu Miyajima[a], Keiko Usui-Kusumoto[a], Peter Sol Reinach[b], Yuka Okada[c], Shizuya Saika[a]

[a] *Department of Ophthalmology, Wakayama Medical University School of Medicine, Wakayama, Japan;* [b] *Department of Ophthalmology and Optometry, Wenzhou Medical University School, Wenzhou, People's Republic of China;* [c] *Department of Ophthalmology, Wakayama Medical University Kihoku Hospital, Wakayama, Japan*

ARTICLE INFO

Article history:
Received 8 March 2022
Revised 20 July 2023
Accepted 28 August 2023
Available online 4 October 2023

Keywords:
bone marrow transplantation
choroidal neovascularization
interleukin 6
neutrophil
transforming growth factor β1
transient receptor potential ankyrin 1

ABSTRACT

We examined the effects of gene ablation and chemical inhibition of transient receptor potential ankyrin 1 (TRPA1) on the growth of experimental argon laser–induced choroidal neovascularization (CNV) in mice. CNV was induced in the eyes of 6- to 8-week-old TRPA1-null (knockout [KO]) and wild-type (WT) mice by argon laser irradiation. Gene expression analysis was performed in laser-injured tissues at days 1 and 3. CNV growth was evaluated at day 14. Reciprocal bone marrow transplantation was performed between each genotype to identify the components responsible for either recipient tissue or bone marrow–derived inflammatory cells. Our results show that laser irradiation successfully induced CNV growth at the site of laser injury. The size of induced CNV was significantly smaller in KO mice than in WT mice at day 14, as determined by angiography with fluorescein isothiocyanate-dextran. Invasion of neutrophils, but not macrophages, was suppressed in association with suppression of the expression of transforming growth factor β1 and interleukin 6 in laser-irradiated KO tissue. Bone marrow transplantation indicated that the genotype of the recipient mouse, but not of inflammatory cells, is attributable to the KO phenotype. Systemic administration of a TRPA1 antagonist also reduced the CNV in a WT mouse. In conclusion, TRPA1 signaling in local cells is involved in growth of laser-induced CNV. The phenotype was not attributable to vascular endothelial cells and inflammatory cells. Blocking TRPA1 signal may therefore be a potential treatment strategy for CNV-related ocular diseases.

Introduction

Choroidal neovascularization (CNV) (also called macular neovascularization) and fibrotic tissue formation in subretinal and/or choroidal tissue are the major features of the exudative form of age-related macular degeneration.[1,2] Hemorrhage or plasma exudation derived from CNV in the subretinal and/or choroidal space significantly impairs the function of a macular retina,

The abstract of the current study was presented by Dr Usui at the Annual Meeting of the Association for Research in Vision and Ophthalmology; April 29–May 3, 2018; Honolulu, Hawaii.

* Corresponding author.
E-mail address: iwanishi@wakayama-med.ac.jp (H. Iwanishi).

0023-6837/$ - see front matter © 2023 United States & Canadian Academy of Pathology. Published by Elsevier Inc. All rights reserved.
https://doi.org/10.1016/j.labinv.2023.100256

leading to severe visual disturbance.[3] The exact mechanism of development of CNV has not yet been clarified. However, involvement of chronic local inflammation against abnormal subretinal deposits (so-called drusen) has been proposed.[4] Intracameral administration of antivascular endothelial cell growth factor (VEGF) antibody exerts a prominent therapeutic effect on the exudative form of CNV by inhibiting the growth of neovascularization and suppressing subretinal plasma exudation, which clearly indicates that the pathobiology of the lesion is dependent on VEGF activity.[5-7] However, the development of new treatment strategies is necessary for cases refractory to anti-VEGF therapy.[8-10]

Mouse models of CNV induced by argon lasers mimic human CNV lesions. In these models, lesions exhibit the same abnormal neovascularization associated with inflammation and fibrotic tissue formation.[11-13] Although the major cellular component of CNV includes vascular cells (vascular endothelial cells and pericytes) and fibrogenic cells, inflammatory or immune cells reportedly play critical roles in the development of neovascular tissue in human cases.[14-19] Neutrophils also play critical roles in the pathology of CNV. The activity of circulating neutrophils and the neutrophil-to-lymphocyte ratio are also involved in the pathology of CNV.[20-24]

Non-VEGF components such as growth factor/cytokine-signaling cascades are also reportedly involved in the development of CNV. For example, mice lacking c-Jun N-terminal kinase 1 exhibit suppression of growth of laser-induced CNV.[25] Despite the fact that blocking transforming growth factor β (TGFβ)/Smad3 signal accelerates in vitro angiogenic activity of vascular endothelial cells, we previously reported that the loss of Smad3 attenuates laser-induced CNV development in association with suppression of local inflammation in mice.[26]

There is cross-talk between growth factor/cytokine-signaling cascades and signaling cascades derived from members of the transient receptor potential (TRP) family. The TRP family consists of TRP vanilloid (TRPV), TRP ankyrin (TRPA1, 3-6), and TRP melastatin (TRPM), among others.[27-30] TRPV, TRPA, or TRPM are further divided into specific members, including TRPV1-6, TRPA1, and TRPM1-8. They are activated by exposure to specific internal or external ligands, specific temperature ranges or mechanical stress, and other such stimuli. [27-30] We have examined the tissue response in the cornea of mice that lack TRPV1, TRPV4, or TRPA1 to determine whether the loss of TRP-derived signaling attenuates growth factor/cytokine-signaling cascades.[31-34] We reported that losing or blocking each of these TRPs suppresses local tissue inflammation in association with suppression of TGFβ signal in alkali-burned mouse corneas.[31-34] Our previous in vitro study showed that the activation of TRPA1 with allyl isothiocyanate did not induce human umbilical vein endothelial cell proliferation and migration. However, supplementing a TRPA1 inhibitor to culture medium blocked tube-like tissue formation by vascular endothelial cells cultured on a fibroblast feeder layer, while VEGF-A signaling was not affected by pharmacologic inhibition of TRPA1.[35] We therefore concluded that cells surrounding the endothelial cells were responsible for TRPA1-mediated new vessel-like tissue formation. These findings suggest that the loss or inhibition of TRPA1 inhibits the growth of laser-induced CNV, another vision-threatening disease, via TRPA1 activity reduction in cells other than vascular endothelial cells in mice.

In the present study, we investigated the effect of gene deletion or chemical inhibition of TRPA1 on the development of laser-induced CNV in mice. We show here that the loss of TRPA1 attenuates the development of laser-induced CNV and that the effect is attributable to the genotype of tissue cells but not to that of bone marrow (BM)–derived cells.

Materials and Methods

Experiments were approved by the DNA Recombination Experiment Committee and the Animal Care and Use Committee of Wakayama Medical University and were performed in accordance with the Association for Research in Vision and Ophthalmology Statement for the Use of Animals in Ophthalmic and Vision Research.

Experimental Choroidal Neovascularization Mouse Model

Argon laser–induced CNV was induced in C57Bl/6 (wild-type [WT]) mice as previously described.[26] Ocular fundus in each eye received argon laser photocoagulation under slit lamp microscope observation. A coverslip was applied to the cornea to facilitate observation of the retina with sodium hyaluronate. Four coagulated lesions were produced using a power of 200 mW, a spot size of 80 μm, and a duration of 0.05 ms. Lesions were located at the 3-, 6-, 9-, and 12-o'clock meridians centered on the optic nerve and were located 2 or 3 disc diameters from the optic nerve. At days 3 ($n = 3$), 5 ($n = 3$), and 7 ($n = 3$) after argon laser irradiation, we checked the expression of CD31 by immunohistochemistry, as described further.[26]

Each eye was enucleated and fixed in 4% paraformaldehyde for 1 hour. The anterior segment (cornea and iris), crystalline lens, and retina were removed from the eyeball. The remaining tissue of the sclera and choroid was flat- mounted after several relaxing radial incisions and a cover slip was applied. Hematoxylin and eosin staining and immunofluorescent staining were performed with anti-CD31 (MEC 13.3) antibody (1:100, sc-18916; Santa Cruz Biotechnology, Inc) as primary antibodies. Secondary antibodies used were anti-rat immunoglobulin G–fluorescein isothiocyanate (FITC) (1:100 in phosphate-buffered saline [PBS], sc-2011; Santa Cruz Biotechnology, for CD31 staining). After overnight treatment with each primary antibody, the specimens were incubated for 2 hours at room temperature with secondary antibodies. All samples were mounted (Vectashield Mounting Medium with DAPI, Vector Lab), and photomicrographs were captured with a digital camera mounted on a fluorescence microscope (Apotome.2, Carl Zeiss).

Quantitation of the Size of Choroidal Neovascularization Lesions in TRPA1-Null (Knockout) and Wild-Type Mice

We then analyzed the effect of the loss of TRPA1 on the development of laser-induced CNV. Our previous study showed that CNV size peaked at day 14 in the current model.[26] Fourteen days after ocular fundus laser photocoagulation in both eyes of C57BL/6-background knockout (KO) mice ($n = 5$) and WT mice ($n = 5$), all 4 laser spots in each eye were subjected to fluorescein-dextran angiography to quantify the size of the CNV lesions. (There were a total of 40 laser irradiation spots in each group.) The size of CNV angiography in choroidal flat mounts was measured as previously reported.[26] In brief, the CNV lesion was visualized with FITC-dextran angiography; FITC-dextran (1 mL/mouse, 50 mg/mL; 2×10^6 MW; 10% dextran, FITC:PBS = 1:1; Sigma) was introduced into the cardiac cavity according to our previous publication.[8] The mice were sacrificed, and the eyes were excised.[8] CNV was then

observed using an Apotome.2 fluorescent microscope (Zeiss).[8] The hyperfluorescent CNV tissue was measured using the software of WinROOF (Mitani),[8] and the total size of CNV lesions per eye was determined as their sum.[8] In brief, FITC was used to visualize CNV (shown in green color), and the area of the vessels that stained was determined. A 2-sample Student's *t* test with unequal variance was used for statistical analyses of the quantitative CNV lesion size in flat-mounted specimens. The effect of the loss of either TRPV1 or TRPV4 on the development of CNV was also examined and compared with data on WT mice (n = 5; 40 laser spots). Fourteen days after ocular fundus laser photocoagulation in both eyes of C57BL/6-background TRPV1-null mice (TRPV1-KO; n = 5), TRPV4-null mice (TRPV4-KO; n = 5), and WT mice (n = 5), all 4 laser spots in each eye were processed for the assay of laser-induced CNV as described above. Data were analyzed using analysis of variance.

Expression Patterns of Inflammation/Wound Healing–Related Components in Laser-Irradiated Tissues

In order to understand the effects of the absence of TRPA1 on the degree of local tissue inflammation and angiogenic activity, we performed gene or protein expression analysis in the laser-irradiated eyes using immunohistochemistry or real-time reverse-transcription PCR (RT-qPCR).[26]

Localization of inflammatory cells in the tissue was determined by immunohistochemistry for neutrophils or macrophages with anti-LY6B.2 antibody or anti-F4/80 antibody. WT and KO mice (n = 6 in each genotype) were used. After argon laser irradiation, the mice were sacrificed at day 1 and day 3. The flat-mounted chorioretinal tissue was processed for immunostaining with anti-LY6B.2 antibody (1:100, MCA771G; Biorad) or anti-F4/80 antibody (1:100, cat # sc-377009; Santa Cruz Biotechnology Inc).

We also immunostained paraffin sections of day 1 WT and KO specimens (n = 3 in each genotype) with TGFβ1 (goat polyclonal, sc-146, X100; Santa Cruz Biotechnology), macrophage chemoattractant protein-1 (MCP-1) (mouse monoclonal, 66272-1-1g, X100; Proteintech), and interleukin 6 (IL-6) (rat monoclonal, X100; R & D). Antibody detection was performed with donkey anti-rat immunoglobulin G (H+L) highly cross-adsorbed secondary antibody, Alexa Fluor 488 (X100; Invitrogen).

Real-Time Reverse-Transcription PCR

We then semiquantified expression using real-time RT-qPCR. We used both eyes of 20 adult WT or 20 KO mice for CNV induction for examinations at day 1 and day 3. Twenty-five laser spots were prepared in each eye. At day 1 (20 eyes in each genotype of mice) and day 3 (20 eyes in each genotype of mice), the mice were sacrificed by cervical dislocation and each eye was enucleated. The tissue of the retinal pigment epithelial-choroid-sclera complex was obtained as previously reported. Four samples of tissue were merged into 1 RNA sample. The expression levels of TGFβ1, myeloperoxidase (MPO) (neutrophil marker), F4/80 (macrophage marker), MCP-1, IL-6, and VEGF-A and α-smooth muscle actin (αSMA) were assayed with real-time RT-qPCR (TaqMan, Propriety Gene Expression Assays; Applied Biosystems). The data were normalized for the endogenous expression of glyceraldehyde-3-phosphate dehydrogenase using $\Delta\Delta C_t$ and were statistically analyzed with the Mann-Whitney *U* test.

Western Blotting for α-Smooth Muscle Actin in Laser-Irradiated Tissues

Detection of αSMA protein was achieved using western blotting. WT and KO mice (n = 5 in each genotype) were used. After argon laser irradiation of 25 spots as described above, the mice were sacrificed at day 14. The chorioretinal tissue was treated with tissue lysis buffer (Sigma) and processed for western blotting with anti-αSMA antibody (Mouse # MS-113, 1:1000; Epredia) or anti-β-actin antibody (1:20,000, Mouse #sc-47778; Santa Cruz). Protein detection was performed with KIT (Immobilon Western Chemiluminescent HRP Substrate, cat # WBKLS0100; Millipore) and observed using ChemiDoc XRS+ System (Bio-Rad Laboratories).

Bone Marrow Transplantation and Laser-Induced Choroidal Neovascularization

Reciprocal bone marrow transplantation (BMT) between mice of each genotype was performed as previously reported.[31-34] Briefly, BM cells were obtained by flushing the tibia and femur of KO (n = 10) and WT (n = 5) mice with PBS. BM cell suspension was injected via tail vein infusion into recipient mice that had received whole-body irradiation of 12 Gy prior to BMT (from WT mice to KO mice or vice versa and from WT mice to WT mice). We checked for chimeric conditions as previously reported.[31-34] The mice in which BM engraftment failed could not survive. The mice were subjected to ocular fundus laser irradiation in each eye, as described above, 4 weeks after BMT. Five eyes with 4 laser spots in each were prepared in 3 groups. The size of CNV was evaluated at day 14, as described above. Data were analyzed using a 2-sample Student's *t* test.

Treatment of Laser-Induced Choroidal Neovascularization in Wild-Type Mice With Systemic TRPA1 Antagonists

We examined whether the KO phenotype is reproduced by intraperitoneal injection of a TRPA1 antagonist into a WT mouse (40 spots in 5 mice for each test or control group) after argon laser irradiation. The antagonist, HC-030031 (100 mg/kg in PBS, daily), or the vehicle (PBS) was administered daily until euthanasia at day 14. Eyes were then processed for fluorescein angiography and evaluation of the size of the CNV as described above. Data were analyzed using the Mann-Whitney *U* test.

Results

Experimental Choroidal Neovascularization Model in Wild-Type Mice

Argon laser irradiation successfully induced CNV in WT mice. FITC-CD31–labeled CNV was easily observed as early as day 3 and increased until the interval examined (up to day 14) in flat-mounted specimens (Fig. 1).

The Size of Choroidal Neovascularization in Knockout Mice

In WT mice, CNV was induced by fundus laser irradiation as early as day 3. We then evaluated the effect of the loss of TRPA1 in day 14 samples with fluorescein-dextran angiography. The size of CNV was significantly smaller in a KO mouse than in a WT mouse

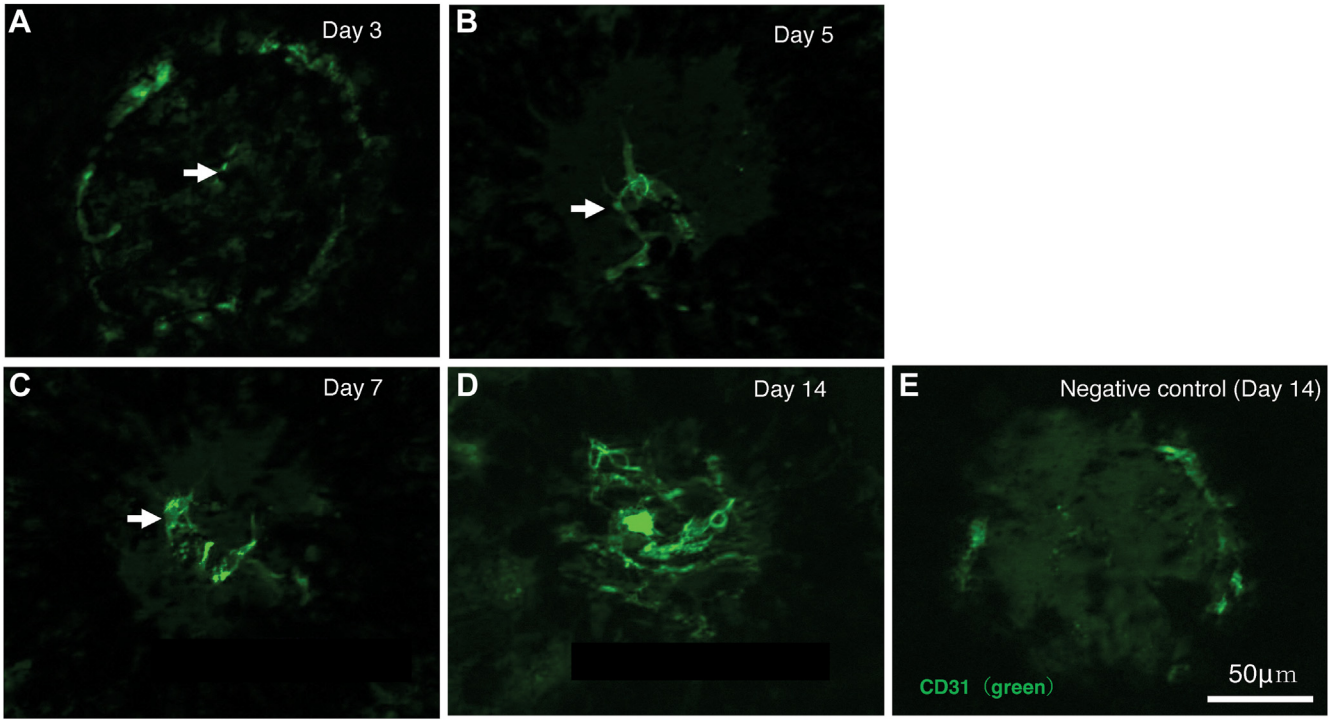

Figure 1.
Development of laser-induced choroidal neovascularization in a C57BL6 (wild-type) mouse. At day 3, (A) fluorescein isothiocyanate–labeled choroidal neovascularization (arrows) can be observed, and it increases on days (B) 5, (C) 7, and (D) 14. (E) Negative control in a day 14 specimen shows no specific staining. Scale bar: 100 μm.

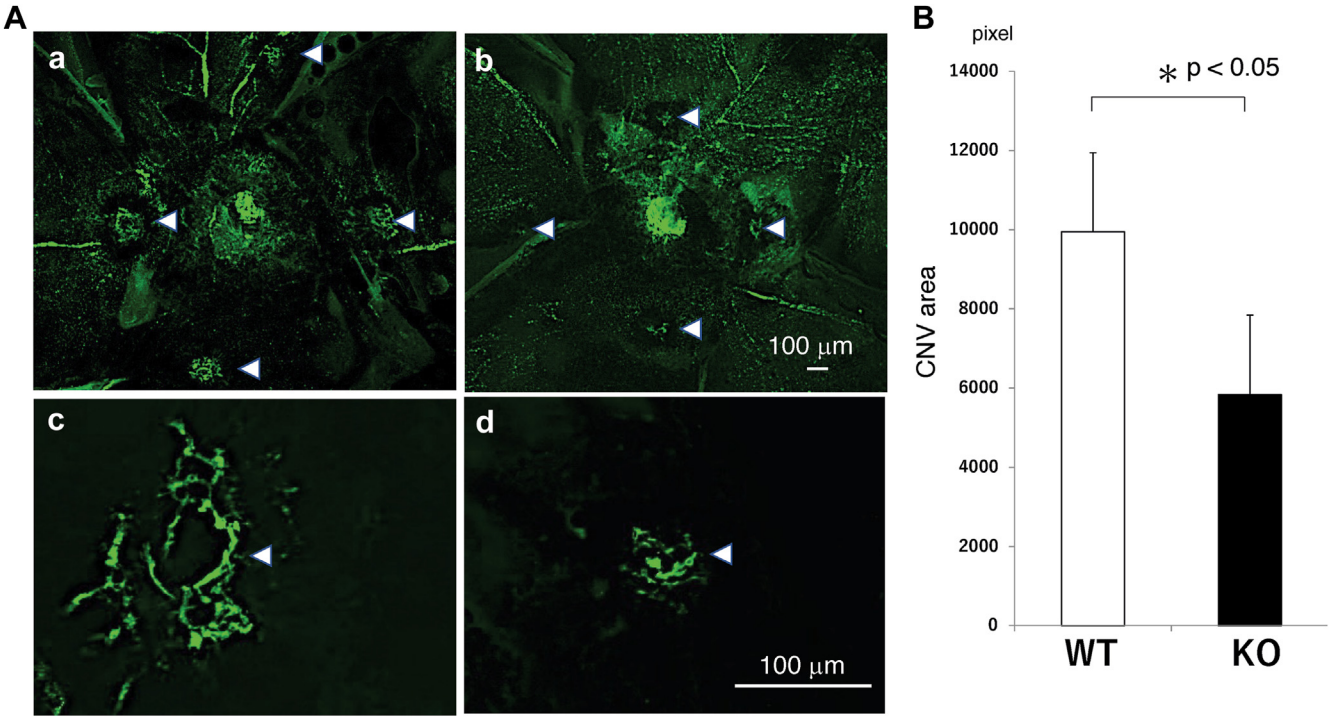

Figure 2.
The loss of transient receptor potential ankyrin 1 attenuates the development of laser-induced choroidal neovascularization (CNV). (A) Fluorescein isothiocyanate–labeled dextran angiography in choroidal flat-mounted specimens showed the growth of CNV (arrowheads) in both wild-type (WT, a and c) and transient receptor potential ankyrin 1–deficient (knockout [KO], b and d) mice at day 14. Arrowheads in subpanels a and b indicate that 4 laser spots were prepared in an ocular fundus. The size of fluorescein isothiocyanate–labeled CNV appears smaller in (d) KO tissue compared than in (c) WT tissue at day 14. Scale bar: 100 μm. (B) Computer software–assisted analysis shows that the size of CNV is significantly smaller in KO tissue than in WT ones. The Y axis indicates the area of CNV as total pixels measured. Bars, SEM; $*P < .05$ by the Student's t test.

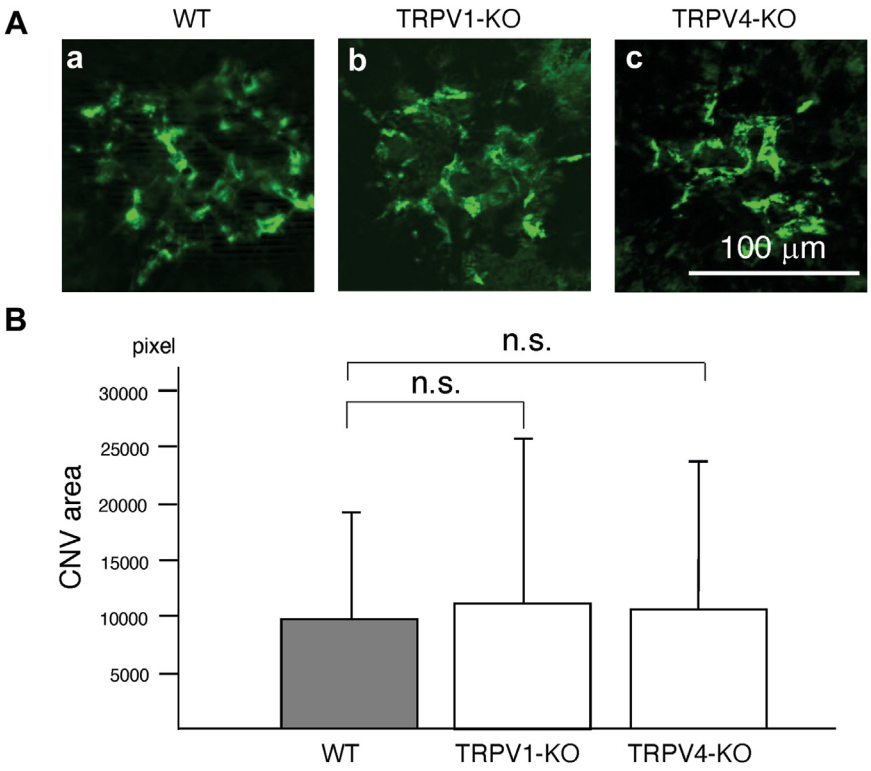

Figure 3.
The loss of transient receptor potential vanilloid (TRPV)1 or TRPV4 does not attenuate the development of laser-induced choroidal neovascularization (CNV). C57BL/6-backgroud TRPV1-null (TRPV1-knockout [KO]) mice (n = 5; b), TRPV4-null (TRPV4-KO) mice (n = 5; c), and wild-type (WT) mice (n = 5; a) were processed for ocular fundus laser photocoagulation and evaluation of the size of the CNV lesions using fluorescein-dextran angiography. (A) Fluorescein angiography shows the growth of CNV in WT, TRPV1-KO, and TRPV4-KO mice. (B) The size of fluorescein isothiocyanate–labeled CNV was similar between WT and each of KO mice. Scale bar: 100 μm. The Y axis indicates the area of CNV as total pixels measured. Bars, SEM; n.s., not significant by the Student's *t* test.

at day 14 (Fig. 2). On the other hand, the loss of TRPV1 or TRPV4 did not attenuate the development of laser-induced CNV (Fig. 3).

Inflammatory Cell Infiltration in Laser-Irradiated Tissues

We first observed the distribution of neutrophils and macrophages in the laser-irradiated area using immunohistochemistry with anti-LY-6B.2 antibodies or anti-F4/80 antibodies. LY-6B.2–labeled neutrophils were detected in laser-treated areas in both genotypes of mice (Fig. 4A). At both day 1 (Fig. 4Aa, Ac) and day 3 (Fig. 4Ab, Ad), the population of neutrophils seemed to be smaller in TRPA1-null (KO) mice than in WT mice. The distribution of F4/80-labeled macrophages in the irradiated areas looked similar between WT and KO mice at both day 1 and day 3 after treatment (Fig. 4B).

Because immunodetection of cells is not a precise quantification, we performed real-time RT-qPCR for cell markers. mRNA expression levels of MPO, a neutrophil marker, and F4/80, a macrophage marker, in chorioretinal tissue were evaluated at day 1 and day 3. The loss of TRPA1 suppressed expression of MPO mRNA at day 3 as compared with a WT mouse (Fig. 4C). TRPA1 gene KO did not affect the expression of F4/80 mRNA both at day 1 and day 3 (Fig. 4D).

Hematoxylin and Eosin Histology

The tissue in the area of laser irradiation at day 1 was histologically observed using hematoxylin and eosin staining. There were no obvious differences between the 2 genotypes (Fig. 5). Thus, we then compared tissue responses to laser irradiation between genotypes by immunohistochemistry and real-time RT-qPCR.

Expression of Angiogenic Factors

Protein expressions of TGFβ1, MCP-1, and IL-6 were evaluated using immunohistochemistry. Slight accumulation of TGFβ1 was observed in the laser-injured tissues. There was no obvious difference in immunoreactivity for these 3 components in tissues (Fig. 6Aa-Af). Because such growth factors are distributed widely in the injured tissue after secretion by the local cells, we semi-quantified the mRNA expression levels of these factors using real-time RT-qPCR (Fig. 6B). mRNA expressions of TGFβ1 and IL-6 were less marked in a KO tissue than in a WT one at day 1 after laser irradiation. mRNA expression levels of MCP-1 and VEGF-A are not altered by the loss of TRPA1.

Expression of α-Smooth Muscle Actin in Laser-Irradiated Chorioretinal Tissues

mRNA expression of SMA in the laser-irradiated chorioretinal tissues at day 1 and day 3 was not significantly affected by the loss of TRPA1 as compared with the WT tissues as evaluated by real-time RT-qPCR (Fig. 6B). Protein detection of αSMA as detected

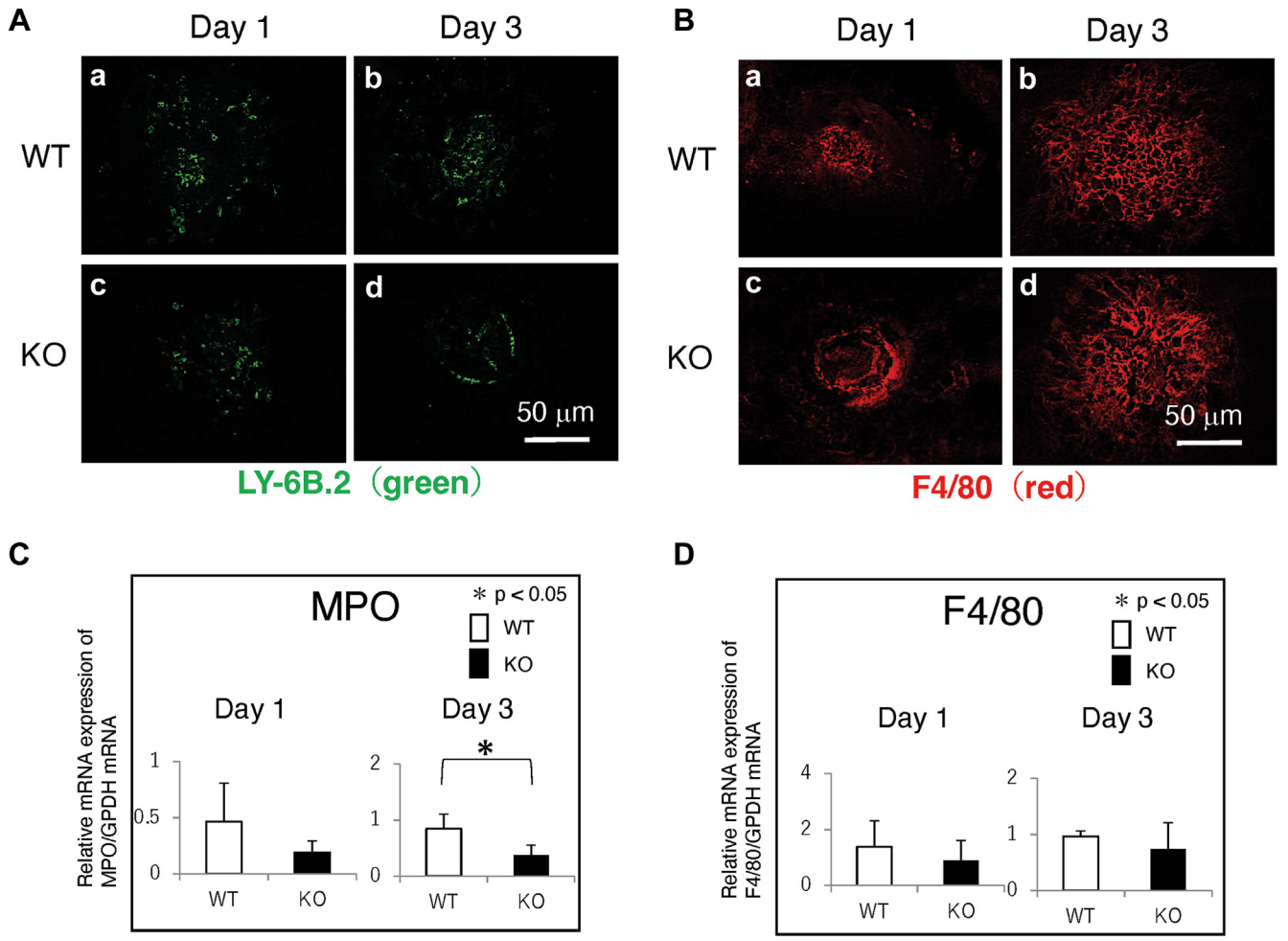

Figure 4.
The loss of transient receptor potential ankyrin 1 (TRPA1) suppresses local accumulation of neutrophils but not macrophages. (A) Ly6B.2-labeled neutrophils are detected in laser-treated areas in both genotypes of mice. At both (a, c) day 1 and (b, d) day 3, the population of neutrophils appears smaller in (c, d) TRPA1-null (knockout [KO]) mice as compared with that in (a, b) wild-type (WT) mice. (B) The distribution of F4/80-labeled macrophages in the irradiated areas is similar between (a, b) WT and (c, d) KO mice at both (a, c) day 1 and (b, d) day 3 after treatment. Scale bar: 50 μm. (C) The messenger RNA expression level of myeloperoxidase, a neutrophil marker, is suppressed by the loss of TRPA1 at day 3 after laser irradiation. (D) Expression of F4/80 macrophage antigen is similar between WT and KO mice. *$P < .05$ by Mann-Whitney U test; bar, mean ± SEM. GPDH, glycerol-3-phosphate dehydrogenase; MPO, myeloperoxidase; mRNA, messenger RNA.

using western blotting was also not affected by TRPA1 gene KO at day 14 (Fig. 6B).

Choroidal Neovascularization Development in Mice After Bone Marrow Transplantation

The size of CNV was significantly smaller in a KO mouse that had received WT or KO BM cells as compared with a WT mouse with transplantation of either WT or KO BM cells (Fig. 7). This finding indicates that the genotype of the recipient mouse, but not of BM-derived inflammatory cells, is attributable to the KO phenotype of suppression of the growth of CNV.

Effect of Treatment of Laser-Induced Choroidal Neovascularization With Systemic TRPA1 Antagonists

Daily administration of a TRPA1 antagonist, HC-030031, successfully reduced the size of the argon laser–induced CNV in WT mice (Fig. 8).

Discussion

In the present study, we showed that the loss of TRPA1 reduced the size of laser-induced CNV in mice for the first time. Immunohistochemistry showed that neovascular tissue itself does not express TRPA1, while this protein was abundantly detected in the cells accumulated in the laser-injured tissue. Gene expression analysis demonstrated that the loss of TRPA1 significantly suppressed infiltration of neutrophils and reduction of expression of TGFβ1 and IL-6 in local tissues. The involvement of TRPA1 signaling in local inflammation and neovascularization has been previously reported.[35,36] Systemic administration of a TRPA1 inhibitor blocks progression of neurogenic pancreatitis from acute phase to chronic one in mice.[37] Similarly, adjuvant-induced arthritis and its related pain behaviors are suppressed by the loss of TRPA1 gene in mice.[38] These previous reports, as well as our current data, support that modulation of TRPA1 exerts therapeutic potential in neovascular diseases in nonocular tissues. The KO phenotype was well reproduced by systemic administration of a TRPA1 antagonist, HC-030031. This suggests the possibility of future development of a treatment strategy by applying some TRPA1 antagonist.

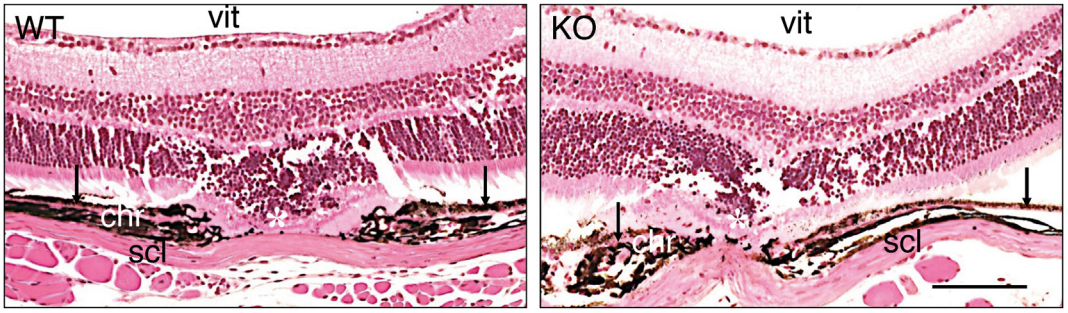

Figure 5.
Hematoxylin and eosin staining histology. The tissue of the area of laser irradiation at day 1 was histologically observed using hematoxylin and eosin staining. There was no obvious difference in histology between the 2 genotypes. Asterisks indicate the center of the laser irradiation spot; arrows indicate the retinal pigment epithelium. chr, choroidal tissue; KO, knockout; scl, sclera; vit, vitreous cavity; WT, wild-type; scale bar: 100 μm.

Knockout Phenotype and Suppression of Neutrophil Infiltration

Neutrophils are involved in the development of neovascularization.[20-24] It was reported that TRPA1 signal is involved in neutrophil infiltration, although this cell type lacks TRPA1.[32,33]

This suggests that absence of TRPA1 in tissue is critical to suppress neutrophil invasion in the laser-irradiated tissue. Such a notion was further supported by current data suggesting that lack of TRPA1 in the recipient mouse was attributable to the inhibition of CNV growth regardless of the genotype of BM cells. A similar finding was observed in a model of cornea alkali burn; suppression of inflammation in the corneal stroma induced by alkali exposure in a mouse that lacks TRPA1 also depends on its loss in tissue but not on BM-derived inflammatory cells.[32]

We reported that the loss of TRPA1 attenuates neovascularization in a mouse cornea despite that immunohistochemistry did not detect TRPA1 in endothelial cells of new vessels.[35] Our previous study showed chemical inhibition of TRPA1 function blocks vessel-like tube formation by vascular endothelial cells cultured on a fibroblast feeder layer, although the activation of TRPA1 signal did not induce human umbilical vein endothelial cell proliferation and migration.[35] These findings suggest that the loss or inhibition of TRPA1 inhibits neutrophil recruitment in the

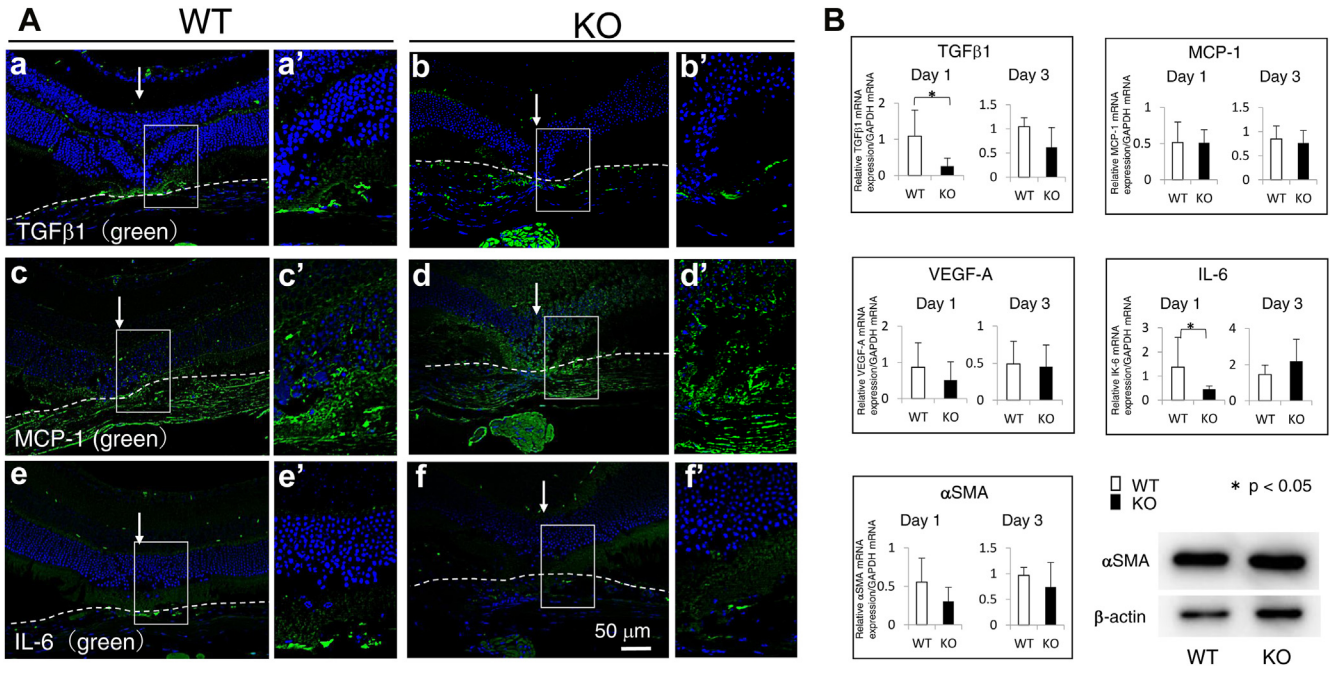

Figure 6.
The loss of transient receptor potential ankyrin 1 (TRPA1) suppresses the messenger RNA (mRNA) expression of transforming growth factor β1 (TGFβ1) during the development of laser-induced choroidal neovascularization. (A) Accumulation of inflammation-related growth factors was faintly observed in the laser-injured tissues using immunohistochemistry. There was no obvious difference in the immunoreactivity for (a, a', b, and b') TGFβ1, (c, c', d, and d') macrophage chemoattractant protein-1 (MCP-1), and (e, e', f, and f') interleukin-6 (IL-6) between tissues of (a, c, and e) wild-type (WT) and (b, d, and f) knockout (KO) mice. Subpanels a' to f' indicate the higher magnification pictures of the boxed areas in subpanels a to f. Arrows indicate the laser-irradiated points. White dotted lines mark the border of the choroid/retinal pigment epithelial complex and subretinal space. Scale bar: 50 μm. (B) mRNA expressions of TGFβ1 and IL-6 as examined using real-time reverse-transcription PCR were less marked in a TRPA1-null (KO) tissue than in a WT one at day 1 after laser irradiation. (e) The expression level of MCP-1, vascular endothelial growth factor-A (VEGF-A), and α-smooth muscle actin (αSMA) was not altered by the loss of TRPA1. *$P < .05$ by Mann-Whitney U test; bar, mean ± SEM. (f) Protein detection of αSMA as detected using western blotting was also not affected by TRPA1 gene knockout on day 14. There was no difference in the αSMA protein level based on western blotting.

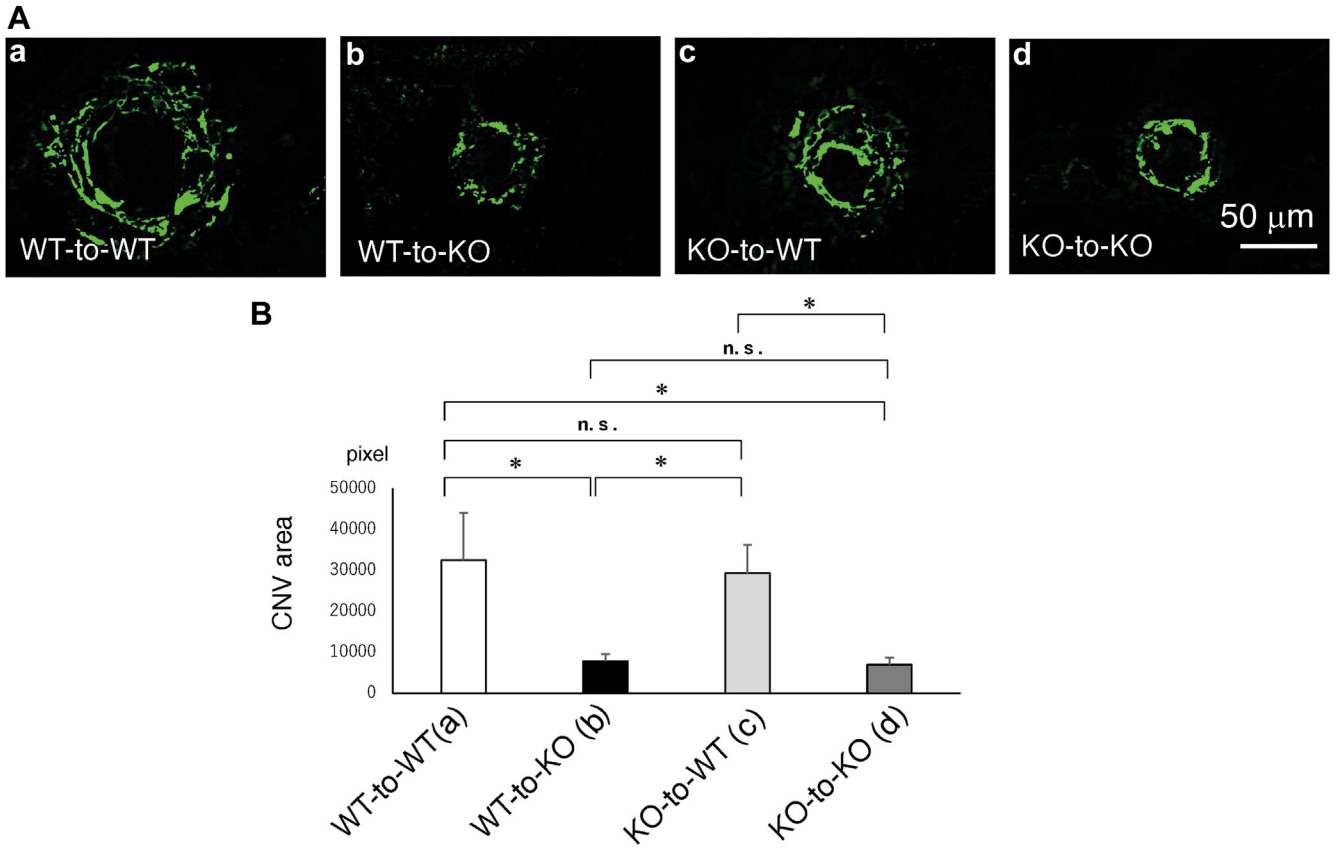

Figure 7.
Growth of laser-induced choroidal neovascularization (CNV) in mice that received reciprocal bone marrow transplantation. (A) Fluorescein isothiocyanate–labeled dextran angiography in choroidal flat-mounted specimens shows the growth of CNV in each group of mice. Scale bar: 50 μm. (B) The size of CNV was significantly smaller in a TRPA1-null (knockout [KO]) mouse that had received wild-type (WT) or KO bone marrow cells (WT-to-KO [b] or KO-to-KO [d]) than in a WT mouse with transplantation of either WT bone marrow (WT-to-WT [a]) or KO bone marrow (KO-to-WT [c]). The Y axis indicates total pixels measured. Bars, SEM; *$P < .05$, by analysis of variance; bar, mean ± SEM. n.s., not significant.

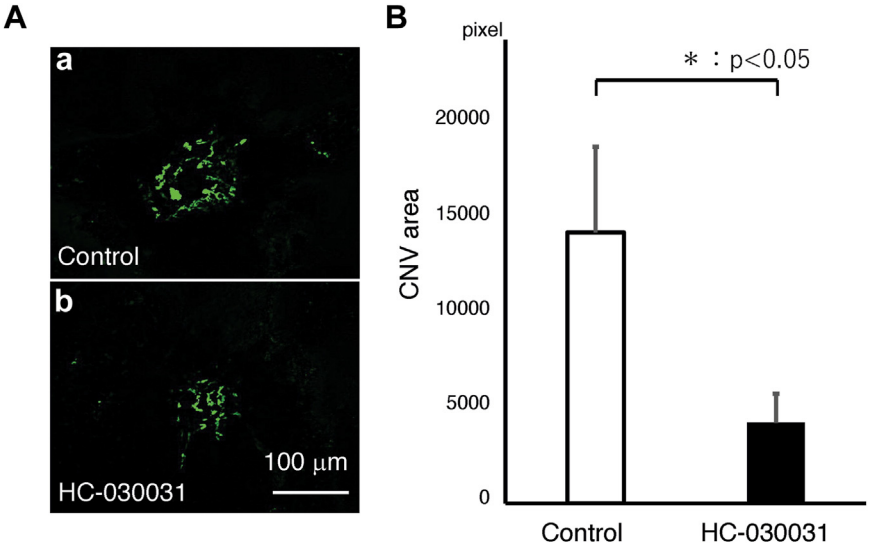

Figure 8.
Effect of systemic administration of a transient receptor potential ankyrin 1 antagonist, HC-030031, on the growth of laser-induced choroidal neovascularization (CNV) in mice. (A) Intraperitoneal administration of injection of a transient receptor potential ankyrin 1 antagonist (b) suppressed the growth of argon laser–induced CNV as compared with that in a (a) mouse with a control vehicle. Scale bar: 100 μm. (B) Statistical analysis showed the significantly smaller CNV with the antagonist as compared with the vehicle. *$P < .05$ by the Mann-Whitney U test.

laser-injured tissue and the growth of laser-induced CNV via TRPA1 activity reduction in cells except vascular endothelial cells in mice.

Knockout Phenotype and Alteration of Growth Factor Expression Levels: Suppression of Expression of TGFβ1 and IL-6

We previously reported that genetic ablation of Smad3 gene suppressed local tissue inflammation and subsequent CNV development in mice.[26] IL-6 is also involved in the development of CNV lesions.[39,40] The present study shows that TRPA1 gene ablation suppressed expression of TGFβ1 and IL-6 in irradiated tissue, which may explain the phenotype of KO mice.

IL-6 is involved in the formation of subretinal fibrosis associated with CNV development.[41] Expression of αSMA is the hallmark for fibrogenic reaction in an injured or neovascularized tissue. Pericytes of new vessels are capable of transforming the phenotype to myofibroblasts and contribute to the formation of the lesion of age-related macular degeneration or other neovascularized lesions in a Smad2/3-dependent manner.[42,43] In the present study, there was no statistical significance of the mRNA and protein expression level of αSMA in laser-irradiated tissue between WT and KO mice, suggesting that TRPA1 gene ablation might not affect fibrogenic reaction in the laser-irradiated tissues.

VEGF-A is a potent neovascularization-promoting factor. However, VEGF-A expression was not downregulated in laser-irradiated tissue by the loss of TRPA1. Because TRPA1-null macrophages normally express VEGF-A as WT macrophages do,[35] it is understandable that both infiltration of macrophages and VEGF-A expression level were similar between genotypes of mice in the present study.

We previously reported that the loss of TRPV1 or TRPV4 suppresses excess inflammatory reaction and resultant tissue fibrosis/neovascularization in the cornea in mice being similar to the phenotype in a TRPA1-deficient mouse.[31,33] Moreover, experiments using cultured vascular endothelial cells and a mouse model of oxygen-induced retinopathy indicate that both TRPV1 and TRPV4 are involved in the development of retinal neovascularization.[44] However, the size of argon laser-induced CNV was similar between a WT mouse and a mouse that lacks either TRPV1 or TRPV4 at day 14. The difference in phenotype of these KO mice between cornea and CNV is to be investigated.

In conclusion, the present study shows that the loss of TRPA1 suppresses neutrophil infiltration and TGFβ1 expression in the laser-injured local tissue, resulting in the inhibition of the development of CNV in mice. Blocking TRPA1 signal may be a treatment strategy for CNV-related ocular diseases.

Author Contributions

The study was conceived and designed by Y.U., K.U.-K., H.I., and S.S. A TRPA1-deficient mouse was bred by M.M. Laser-induced choroidal neovascularization was analyzed by H.I. Western blotting and immunostaining were analyzed by Y.O. and K.I. Bone marrow transplantation procedures were performed by Y.O. The manuscript writing and figure design were performed by Y.U., H.I., T.S., P.S.R., and S.S. All authors reviewed and accepted the final version of the manuscript.

Data Availability

The data that support the findings of this study are available from the corresponding author (H.I.) upon reasonable request.

Funding

This study was supported by the Grants from the Ministry of Education, Science, Sports and Culture of Japan (16H07135 and 18K16933 [H.I.], 15K10878 and 19K09937 [Y.O.], and C25462729 and 17K11464 [S.S.]) and Wakayama Medical University School of Medicine Internal Research Grant for Young Investigators (Y.U.).

Declaration of Competing Interest

The authors declare that they have no conflict of interest.

Ethics Approval and Consent to Participate

All experiments were approved by the DNA Recombination Experiment Committee and the Animal Care and Use Committee of Wakayama Medical University (protocol number: 956) and performed in accordance with the Association for Research in Vision and Ophthalmology Statement for the Use of Animals in Ophthalmic and Vision Research.

References

1. Yeo NJY, Chan EJJ, Cheung C. Choroidal neovascularization: mechanisms of endothelial dysfunction. *Front Pharmacol*. 2019;10:1363.
2. Zhao S, Lan X, Wu J, et al. Protocol of global incidence and progression of age-related macular degeneration: a systematic review. *Medicine (Baltimore)*. 2019;98(10), e14645.
3. Friedlander M. Fibrosis and diseases of the eye. *J Clin Invest*. 2007;117(3):576–586.
4. Crabb JW, Miyagi M, Gu X, et al. Drusen proteome analysis: an approach to the etiology of age-related macular degeneration. *Proc Natl Acad Sci U S A*. 2002;99(23):14682–14687.
5. Miller JW. Developing therapies for age-related macular degeneration: the art and science of problem-solving: the 2018 Charles L. Schepens, MD, lecture. *Ophthalmol Retina*. 2019;3(10):900–909.
6. Supuran CT. Agents for the prevention and treatment of age-related macular degeneration and macular edema: a literature and patent review. *Expert Opin Ther Pat*. 2019;29(10):761–767.
7. Bird AC. Therapeutic targets in age-related macular disease. *J Clin Invest*. 2010;120(9):3033–3041.
8. Lalwani GA, Rosenfeld PJ, Fung AE, et al. A variable-dosing regimen with intravitreal ranibizumab for neovascular age-related macular degeneration: year 2 of the PrONTO study. *Am J Ophthalmol*. 2009;148(1):43–58.e1.
9. Holz FG, Amoaku W, Donate J, et al. Safety and efficacy of a flexible dosing regimen of ranibizumab in neovascular age-related macular degeneration: the SUSTAIN study. *Ophthalmology*. 2011;118(4):663–671.
10. Daniel E, Toth CA, Grunwald JE, et al. Risk of scar in the comparison of age-related macular degeneration treatments trials. *Ophthalmology*. 2014;121(3):656–666.
11. Montezuma SR, Vavvas D, Miller JW. Review of the ocular angiogenesis animal models. *Semin Ophthalmol*. 2009;24(2):52–61.
12. Grossniklaus HE, Kang SJ, Berglin L. Animal models of choroidal and retinal neovascularization. *Prog Retin Eye Res*. 2010;29(6):500–519.
13. Lambert V, Lecomte J, Hansen S, et al. Laser-induced choroidal neovascularization model to study age-related macular degeneration in mice. *Nat Protoc*. 2013;8(11):2197–2211.
14. Tan X, Fujiu K, Manabe I, et al. Choroidal neovascularization is inhibited via an intraocular decrease of inflammatory cells in mice lacking complement component C3. *Sci Rep*. 2015;5:15702.
15. Ding X, Patel M, Chan CC. Molecular pathology of age-related macular degeneration. *Prog Retin Eye Res*. 2009;28(1):1–18.
16. Nussenblatt RB, Ferris III F. Age-related macular degeneration and the immune response: implications for therapy. *Am J Ophthalmol*. 2007;144(4):618–626.

17. Espinosa-Heidmann DG, Suner IJ, Hernandez EP, Monroy D, Csaky KG, Cousins SW. Macrophage depletion diminishes lesion size and severity in experimental choroidal neovascularization. *Invest Ophthalmol Vis Sci*. 2003;44(8):3586–3592.
18. Sakurai E, Anand A, Ambati BK, van Rooijen N, Ambati J. Macrophage depletion inhibits experimental choroidal neovascularization. *Invest Ophthalmol Vis Sci*. 2003;44(8):3578–3585.
19. Ishikawa K, Kannan R, Hinton DR. Molecular mechanisms of subretinal fibrosis in age-related macular degeneration. *Exp Eye Res*. 2016;142:19–25.
20. Subhi Y, Lykke Sørensen T. New neovascular age-related macular degeneration is associated with systemic leucocyte activity. *Acta Ophthalmol*. 2017;95(5):472–480.
21. Krogh Nielsen M, Hector SM, Allen K, Subhi Y, Sørensen TL. Altered activation state of circulating neutrophils in patients with neovascular age-related macular degeneration. *Immun Ageing*. 2017;14:18.
22. Niazi S, Krogh Nielsen M, Sørensen TL, Subhi Y. Neutrophil-to-lymphocyte ratio in age-related macular degeneration: a systematic review and meta-analysis. *Acta Ophthalmol*. 2019;97(6):558–566.
23. Qi J, Pan W, Peng T, et al. Higher circulating levels of neutrophils and basophils are linked to myopic retinopathy. *Int J Mol Sci*. 2022;24(1):80.
24. Hamada T, Tsuchihashi S, Avanesyan A, et al. Cyclooxygenase-2 deficiency enhances Th2 immune responses and impairs neutrophil recruitment in hepatic ischemia/reperfusion injury. *J Immunol*. 2008;180(3):1843–1853.
25. Du H, Sun X, Guma M, et al. JNK inhibition reduces apoptosis and neovascularization in a murine model of age-related macular degeneration. *Proc Natl Acad Sci U S A*. 2013;110(6):2377–2382.
26. Iwanishi H, Fujita N, Tomoyose K, et al. Inhibition of development of laser-induced choroidal neovascularization with suppression of infiltration of macrophages in Smad3-null mice. *Lab Invest*. 2016;96(6):641–651.
27. Li H. TRP channel classification. *Adv Exp Med Biol*. 2017;976:1–8.
28. Santoni G, Maggi F, Morelli MB, Santoni M, Marinelli O. Transient receptor potential cation channels in cancer therapy. *Med Sci (Basel)*. 2019;7(12):108.
29. Muller C, Morales P, Reggio PH. Cannabinoid ligands targeting TRP channels. *Front Mol Neurosci*. 2019;11:487.
30. Palazzo E, Rossi F, de Novellis V, Maione S. Endogenous modulators of TRP channels. *Curr Top Med Chem*. 2013;13(3):398–407.
31. Okada Y, Reinach PS, Shirai K, et al. TRPV1 involvement in inflammatory tissue fibrosis in mice. *Am J Pathol*. 2011;178(6):2654–2664.
32. Okada Y, Shirai K, Reinach PS, et al. TRPA1 is required for TGF-β signaling and its loss blocks inflammatory fibrosis in mouse corneal stroma. *Lab Invest*. 2014;94(9):1030–1041.
33. Okada Y, Shirai K, Miyajima M, et al. Loss of TRPV4 function suppresses inflammatory fibrosis induced by alkali-burning mouse corneas. *PLoS One*. 2016;11(12):e0167200.
34. Nidegawa-Saitoh Y, Sumioka T, Okada Y, et al. Impaired healing of cornea incision injury in a TRPV1-deficient mouse. *Cell Tissue Res*. 2018;374(2):329–338.
35. Usui-Kusumoto K, Iwanishi H, Ichikawa K, et al. Suppression of neovascularization in corneal stroma in a TRPA1-null mouse. *Exp Eye Res*. 2019;181:90–97.
36. Zhou Y, Han D, Follansbee T, et al. Transient receptor potential ankyrin 1 (TRPA1) positively regulates imiquimod-induced, psoriasiform dermal inflammation in mice. *J Cell Mol Med*. 2019;23(7):4819–4828.
37. Naert R, López-Requena A, Talavera K. TRPA1 expression and pathophysiology in immune cells. *Int J Mol Sci*. 2021;22(21):11460.
38. Horváth Á, Tékus V, Boros M, et al. Transient receptor potential ankyrin 1 (TRPA1) receptor is involved in chronic arthritis: in vivo study using TRPA1-deficient mice. *Arthritis Res Ther*. 2016;18:6.
39. Droho S, Cuda CM, Perlman H, Lavine JA. Macrophage-derived interleukin-6 is necessary and sufficient for choroidal angiogenesis. *Sci Rep*. 2021;11(1),18084.
40. Lavine JA, Farnoodian M, Wang S, et al. β2-Adrenergic receptor antagonism attenuates CNV through inhibition of VEGF and IL-6 expression. *Invest Ophthalmol Vis Sci*. 2017;58(1):299–308.
41. Sato K, Takeda A, Hasegawa E, et al. Interleukin-6 plays a crucial role in the development of subretinal fibrosis in a mouse model. *Immunol Med*. 2018;41(1):23–29.
42. Natarajan V, Ha S, Delgado A, et al. Acquired αSMA expression in pericytes coincides with aberrant vascular structure and function in pancreatic ductal adenocarcinoma. *Cancers (Basel)*. 2022;14(10):2448.
43. Zhao Z, Zhang Y, Zhang C, et al. TGF-β promotes pericyte-myofibroblast transition in subretinal fibrosis through the Smad2/3 and Akt/mTOR pathways. *Exp Mol Med*. 2022;54(5):673–684.
44. O'Leary C, McGahon MK, Ashraf S, et al. Involvement of TRPV1 and TRPV4 Channels in Retinal Angiogenesis. *Invest Ophthalmol Vis Sci*. 2019;60(10):3297–3309.